Iodate production in cultures of marine ammonia-oxidising bacteria: implications for future inorganic iodine distributions in the oceans

Claire Hughes[1*], Eleanor Barton[1*], Helmke Hepach[1], Rosie Chance[2], Matt Pickering[1], Karen Hogg[3], Andreas Pommerening-Röser[4], Martin R. Wadley[5], David P. Stevens[5] and Tim D. Jickells[6]

[1] Department of Environment and Geography, University of York, Wentworth Way, Heslington, York, YO10 5NG, UK

[2] Wolfson Atmospheric Chemistry Laboratory, Department of Chemistry, University of York, Heslington, York, YO10 5DD, UK

[3] Bioscience Technology Facility, Department of Biology, University of York, Wentworth Way, York, YO10 5DD, UK

[4] University of Hamburg, Mikrobiologie & Biotechnologie, Ohnhorststr. 18, D-22609 Hamburg, Germany

[5] School of Mathematics, University of East Anglia, Norwich Research Park, Norwich, NR4 7TJ, UK

[6] School of Environmental Sciences, University of East Anglia, Norwich Research Park, Norwich, NR4 7TJ, UK

*authors contributed equally to the manuscript

Corresponding author: Claire Hughes (c.hughes@york.ac.uk)

Key points:

- The oxidation of iodide to iodate was observed for the first time in cultures of marine ammonia-oxidising bacteria
- A decline in ammonia-oxidation under ocean acidification could increase sea surface iodide and thus enhance ozone deposition to the ocean

1. Abstract

Reaction with iodide (I^-) at the sea surface is an important sink for atmospheric ozone, and causes sea-air emission of reactive iodine which in turn drives further ozone destruction. To incorporate this process into chemical transport models, improved understanding of the factors controlling marine iodine speciation, and especially sea-surface iodide concentrations, is needed. The oxidation of I^- to iodate (IO_3^-) is the main sink for oceanic I^-, but the mechanism for this remains unknown. We demonstrate for the first time that marine nitrifying bacteria mediate I^- oxidation to IO_3^-. A significant increase in IO_3^- concentrations compared to media-only controls was observed in cultures of the ammonia-oxidising bacteria *Nitrosomonas* sp. (Nm51) and *Nitrosoccocus oceani* (Nc10) supplied with 9-10 mM I^-, indicating I^- oxidation to IO_3^-. Cell-normalised production rates were 15.69 (±4.71) fmol IO_3^- $cell^{-1}$ d^{-1} for *Nitrosomonas* sp., and 11.96 (±6.96) fmol IO_3^- $cell^{-1}$ d^{-1} for *Nitrosococcus oceani*, and molar ratios of iodate-to-nitrite production were 9.2±4.1 and 1.88±0.91 respectively. Preliminary experiments on nitrite-oxidising bacteria showed no evidence of I^- to IO_3^- oxidation. If the link between ammonia and I^- oxidation observed here is representative, our ocean iodine cycling model predicts that decreases in marine nitrification under ocean acidification could lead to significantly higher sea surface I^-. A global sensitivity analysis suggests a 0.13 nM increase in sea surface I^- concentrations per percentage decrease in nitrification rate. In turn, this could result in increased O_3 deposition to the sea surface and sea-air iodine emissions, with implications for atmospheric chemistry and air quality.

2. Introduction

Iodine plays an important role in catalytic ozone destruction and new particle formation in the troposphere, thereby impacting the oxidative capacity of the atmosphere (Sherwen *et al*., 2016) and the Earth's radiation balance (O'Dowd *et al*., 2002). Sea-to-air iodine transfer is known to be the main source of iodine to the atmosphere (Carpenter, 2003; Sherwen *et al.,* 2016). Reactive inorganic iodine (I_2, HOI) emissions resulting from the reaction of gas-phase ozone with sea surface iodide (I^-) is now thought to be the dominant mechanism mediating sea-air iodine emissions (Carpenter *et al*., 2013). The strength of the surface reactive iodine flux is related to sea surface I^- concentrations (Carpenter *et al*., 2013) so knowledge of ocean I^- distributions is required in order to estimate the significance of this process. Furthermore, a detailed understanding of the processes controlling inorganic iodine speciation is needed to allow us to develop predictive capacity regarding sea surface I^-, ozone-deposition rates and sea-air emission of reactive iodine.

Total inorganic iodine is found at 400-500 nM in seawater and predominantly exists as iodate (IO_3^-) and I^- (Chance *et al.*, 2014) with inter-conversion between these two species alongside physical mixing being the main causes of spatial and temporal variability in sea surface I^-. Iodate is the thermodynamically stable form and the dominant form in the deep ocean. The existence of relatively higher levels of I^- in the euphotic zone (reviewed by Chance *et al.,* 2014) has led to the suggestion that IO_3^- reduction to I^- is linked to primary productivity. This theory has been supported by observations of I^- production in cultures of a wide range of marine phytoplankton (e.g. Chance *et al*., 2007; Bluhm *et al*., 2010) and some field studies (Chance *et al.,* 2010). Proposed mechanisms for IO_3^- reduction to I^- by marine phytoplankton include nitrate reductase enzymes (Hung *et al*., 2005) and reactions of iodate with reduced sulphur species exuded from cells during senescence (Bluhm et al., 2010), but neither has yet been confirmed as the dominant route of conversion. I^- oxidation to IO_3^- is also known to occur with rate estimates ranging from ~4 to 670 nM yr^{-1} (reviewed in Chance *et al*., 2014). Abiotic oxidation of I^- back to IO_3^- in the ocean (e.g. by oxygen, hydroxyl radicals,

hydrogen peroxide and ozone) is thought to occur so slowly as to be insignificant (e.g. Wong, 1991), and so I^- oxidation to IO_3^- is also thought to be associated with marine microbiological activity. The rates and processes involved in I^- to IO_3^- oxidation are associated with large uncertainty (Truesdale *et al*., 2001; Amachi *et al*., 2008), and the mechanisms involved remain undefined. This uncertainty has been suggested to be one of the factors hindering the development of mathematical models of iodine transformations in the global oceans (Truesdale *et al*., 2001).

I^- oxidation to I_2 has been observed in bacterial isolates obtained from a range of environments including seawater aquaria (Gozlan *et al*., 1968), natural gas brines (Lino *et al*., 2016) and seawater/marine mud (Fuse *et al*., 2003). Additionally, based on field observations, a number of studies (Truesdale *et al*., 2001; Žic *et al*., 2013) have proposed that I^- oxidation to IO_3^- is linked to nitrification in marine systems. Nitrification is the two-stage biological transformation of ammonia (NH_3) to nitrate (NO_3^-) (Equations 1 and 2; Koops & Pommerening-Röser, 2001) mediated by chemoautotrophic ammonia-oxidising bacteria (AOB), and nitrite-oxidising bacteria (NOB). Previously thought to only occur outside of the euphotic zone, nitrification is now known to occur throughout the oceanic water-column (reviewed by Yool *et al*., 2007).

$$2NH_4^+ + 3O_2 \rightarrow 2NO_2^- + 4H^+ + 2H_2O \quad (1)$$

$$2NO_2^- + O_2 \rightarrow 2NO_3^- \quad (2)$$

A link between I^- oxidation/ IO_3^- production and nitrification is yet to be confirmed but, if established, would suggest that I^- oxidation to IO_3^- is widespread throughout the world's oceans (Yool *et al*., 2007).

The primary aim of this study was to establish whether I^- oxidation to IO_3^- is associated with marine nitrification. Our objectives were to determine if IO_3^- production occurs in cultures of marine ammonia- and nitrite-oxidising bacteria supplied with I^-, determine the relative rates of IO_3^-

production and nitrification, and use an ocean iodine cycling model (Wadley et al., 2020) to establish how predicted future changes in marine nitrification could impact sea-surface iodide fields.

3. Methods

3.1.Cultures

Two AOB cultures (*Nitrosomonas* sp. [Nm51] and *Nitrosococcus oceani* [Nc10]) were investigated for IO_3^- production in the presence of I^- as the only iodine source. Cultures were grown in the dark in a water bath at 25 ^oC in autoclaved ESAW artificial seawater mixture (Berges *et al*., 2001) made up using distilled water. The ESAW media was supplemented with 7-8 mM ammonium chloride and potassium phosphate. We also conducted preliminary tests on three active marine NOB (*Nitrospira marina* [295], *Nitrospina gracilis* [3/211], *Nitrococcus mobilis* [231]) but saw no evidence of IO_3^- production in any of the cultures studied. These results are not discussed further. Handling of cultures was done at all times in a biosafety cabinet using sterile equipment.

3.2. Experimental Set Up

For the AOB experiments triplicate cultures were incubated alongside triplicate media-only controls for periods of 8-12 days. The experiments were kept as short as possible to avoid significant changes in pH in the bulk media which would impact inorganic iodine speciation. Hence experiments were only run until an increase in nitrite across two time-points was observed. Samples were taken at regular intervals of between 1 to 6 days for pH measurement, cell counts and determination of NO_2^-, IO_3^-, I^- and NH_4^+/NH_3 concentrations. In all cases, I^- (Aristar) was added to be at similar concentrations with the NH_4^+ required in the growth media. The levels of I^- are much higher than those encountered in the oceans (global ocean median=77 nM I^- [interquartile range 28-140 nM], Chance *et al*., 2014) but were chosen to be similar to the levels of NH_4^+. This is because in the

marine environment nitrifiers would be exposed to similar ratio of NH_4^+ and I^-. For example, Rees *et al.* (2006) show that NH_4^+/NH_3 occurs at concentrations ranging from 60-300 nM in the Atlantic between 60°N to 50°S.

3.2.1. pH

A spectrophotometric method using a Lambda 25 UV/Vis spectrophotometer (Perkin-Elmer) and m-cresol purple dye (Dickson *et al.*, 2007) with measurements at 730, 578 and 434 nm was used to determine pH in the cultures and media-only controls. Salinity, needed for the pH calculation, was calculated from conductivity measured using a calibrated Hanna Instruments hand-held probe.

3.2.2. Cell counts

Immediately after sampling, 4 mL of the culture was fixed with 15 µL of 50% glutaraldehyde (Alfa Aesar), flash frozen in liquid nitrogen and placed in a -80 °C freezer for later determination of cell density. Cell counts were made using a Beckman Coulter Cytoflex S flow cytometer (flow rate of 10 µL min^{-1}) within 2 months of collection. DAPI (Sigma; 2 µg mL^{-1}) stained samples were excited by a laser at 405 nm and the emitted fluorescence detected using an avalanche photodiode detector with a reflective band pass filter 450/45. The flow cytometer thresholds were set using the 405 nm laser side scatter and the DAPI fluorescence signals.

3.2.3. Nitrite concentration

NO_2^- was measured in 0.45 µm (Millex) filtered samples using a spectrophotometric method (Lambda 25 UV/Vis spectrophotometer, Perkin-Elmer) developed by Norwitz & Keliher (1984). The method involves diazotizing nitrite with sulfanilamide (Fisher, analytical reagent grade) and coupling with N-1-naphthylethylenediamine dihydrochloride (Fisher, analytical reagent grade) to form a

coloured azo dye which is measured spectrophotometrically at 540 nm. The method was calibrated using $NaNO_2$ standards (Fisher, analytical reagent grade) prepared in the ESAW-based media.

3.2.4. Iodate Concentration

IO_3^- concentrations were measured in 0.45 µm (Millex) filtered samples using a manual version of the spectrophotometric (Lambda 25 UV/Vis spectrophotometer) method detailed in Truesdale & Spencer, 1974 and Jickells *et al.*, 1988. Absorbance was measured at 350 nm. Strictly, this method determines all oxidised (0 to +5 oxidation state) forms of inorganic iodine, but in seawater derived media this is predominantly IO_3^-, and so will be referred to as IO_3^- iodate hereafter. The method was calibrated using potassium iodate (Aristar) standard solutions made up in ESAW.

Some validation and modification to the method was required due to the nature of our experimental set-up. Chapman & Liss (1977) show that NO_2^- can interfere with spectrophotometric IO_3^- measurements (using sulfamic acid) at ambient seawater concentrations with a 15% error. Clearly significant interference would be an issue for our experiments where NO_2^- was being produced so we ran tests. We found that the presence of NO_2^- up to 10 µM had negligible impact on IO_3^- measurements (between 0.1-50 µM). We did however identify that the high starting concentration of I^- (~10 µM) in the culture media was problematic. The iodate analysis method comprises two steps: the first involves an initial absorbance reading after the addition of sulphamic acid; the second involves the addition of excess I^-. Under acidic conditions I^- reacts with IO_3^- to form I_2 (equation 3a) which reacts with excess I^- to form the coloured ion I_3^- (equation 3b) that can be measured spectrophotometrically.

$$IO_3^- + 5I^- + 6H^+ \rightarrow 3I_2 + 3H_20 \qquad (3a)$$

$$I_2 + I^- \rightarrow I_3^- \qquad (3b)$$

171 The difference between the first and second absorbance readings is then used to calibrate the method.
172 In the case of our experiments the media already contained excess I^- so the formation of I_2 and I_3^-
173 was initiated as soon as the acid was added in the first step. Hence we calibrated the method based on
174 a single absorbance reading obtained after acid and then additional I^- was added. Calibrations and
175 standard checks revealed this approach did not have any impact on the quality of the data.

176

177 **3.2.5. Ammonium Concentration**

178 NH_4^+ concentrations were measured in 0.45 µm (Millex) filtered samples with a Seal Analytical
179 Autoanalyser 3 according to method G-109-93 rev. 10 (Seal Analytical) using sodium salicylate,
180 dichloro-isocyanuric acid and citrate buffer. The method was calibrated using standards ranging from
181 0-2 mg/L prepared from dilutions of a 1000 mg/L ammonium standard solution (Merck).

182

183 **3.2.6. Iodide Concentration**

184 I^- concentrations were determined using a Dionex ICS-2000 ion chromatograph equipped with an
185 EGC III KOH elugen cartridge, AG18 (2 x 50 mm) guard column, AS18 (2 x 250 mm) analytical
186 column, ASRS 300 (2 mm) suppressor, DS6 heated conductivity cell and AS40 autosampler.
187 Samples were diluted 100-fold with 18 MΩ deionised water for analysis and 5 µL was injected onto
188 the ion chromatograph. Aqueous potassium hydroxide was used as the eluent at a flow rate of 0.25
189 mL min^{-1} with a gradient program starting from an initial concentration of 2 mM hydroxide (hold 1
190 min) to 20 mM at 18 min then to 41 mM at 19 min (hold 2 min) before returning to 2 mM. The I^-
191 retention time was 19 min. The instrument was calibrated with matrix-matched standards ranging
192 from 0-100 nM (I^-), prepared from dilutions of a 1000 mg/L iodide standard solution (Fisher
193 Scientific) with 18 MΩ deionised water and containing a final concentration of 1% ESAW.

194

3.2.7. Data Analysis

As in Guerrero and Jones (1996), the NH_4^+ oxidation rate is defined here as the rate of increase in NO_2^-. Similarly, we define the rate of I^- oxidation as the rate of increase in IO_3^-. This is appropriate as no other iodine species were supplied to the cultures and conversion between I^- and IO_3^- is known to be the main cause of variability in inorganic iodine speciation (Bluhm *et al*., 2010; Chance *et al*., 2014). Average NO_2^- and IO_3^- production rates were calculated for each replicate culture using Equation 4.

$$\text{Production Rate (nM day}^{-1}) = \frac{(C_{end} - C_0)}{t} \quad (4)$$

where C_0 and C_{end} are the NO_2^- or IO_3^- concentrations observed at the start and end of the experiment and t is the experimental duration in days. Cell-normalised rates were calculated by dividing these rates by the final cell density observed in each AOB culture and are hence likely to be minimum values.

3.3. Modelling iodine cycling in the ocean

In a companion paper Wadley *et al.* (2020) develop an ocean iodine cycling model, with iodide production driven by primary productivity, and iodide oxidation to iodate linked to nitrification in the mixed layer. We use nitrogen fluxes derived from a global biogeochemical cycling model (Yool *et al.*, 2007) to derive the spatial distribution of mixed layer ammonia oxidation. Iodide is oxidised to iodate in association with the ammonia oxidation, with the same I:N:C ratio as associated with iodide production (Truesdale *et al*., 2001; Long *et al*., 2015). For full discussion of how the model was optimised for I^- oxidation refer to Wadley *et al*. (2020). The iodine cycling model is embedded within a circulation model of the upper ocean. The model does not include an explicit nitrogen cycle, but uses Redfield ratios to implicitly cycle nitrogen. The partitioning of ammonia oxidation between

nitrification in the mixed layer and nitrification in the ocean interior has been quantified by Yool *et al.* (2007), using a global biogeochemical model, and this partitioning is used in the iodine cycling model.

We use the iodine cycling model to determine the changes in surface I^- concentrations that will result from the future changes in the nitrification rate proposed by Beman *et al*. (2011). The Yool *et al*. (2007) model has been run with three rates of nitrification (0.02, 0.2 [the standard rate] and 2 day^{-1}) giving corresponding global fields for the proportion of ammonia oxidised in the mixed layer (Yool, *personal communication*). These results were interpolated to give the required proportion of ammonia oxidised in the mixed layer for each of our sensitivity runs, in which nitrification rates were perturbed by +10%, -10%, -22% and -44%. In the model a reduction in the nitrification rate results in a reduction in the oxidation of ammonia to nitrite, and a corresponding reduction in the oxidation of iodide to iodate (see Wadley *et al*., 2020 for details).

4. Results

4.1. Cell counts and pH

Increases in cell density were observed in all replicates of *Nitrosomonas* sp. and *Nitrosococcus oceani* between the start and end of the experiment indicating growth (Figure 1). Average initial cell density in the *Nitrosomonas* sp. cultures was 21,767 (±4,046) cells mL^{-1} and this increased to 150,983 (±7,585) cells mL^{-1} by the end of the experiment (8 days). For *Nitrosococcus oceani* start and end (12 days) cell densities were 16,947 (± 3,098) and 71,430 (±9,062) cells mL^{-1}, respectively. Average pH levels in the culture experiments calculated from measurements at each time point (data not shown) were 7.69 (±0.07) for *Nitrosomonas* sp. and 7.41 (±0.12) for *Nitrosococcus* sp. These pH levels are consistent with those found in the media-only controls (7.64±0.07 for *Nitrosomonas* sp; 7.64±0.15 for *Nitrosococcus oceani*).

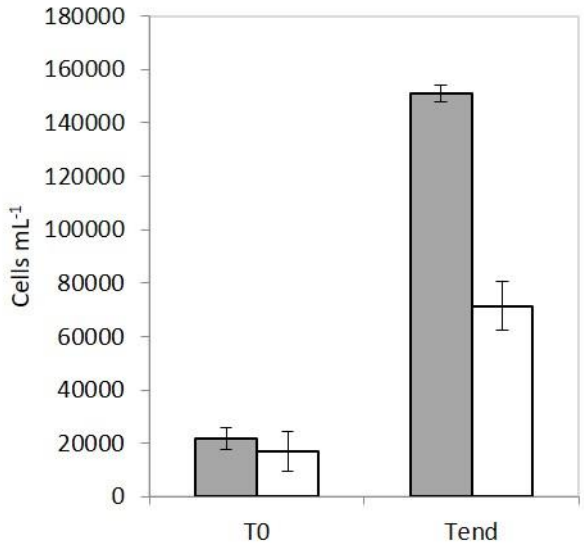

Figure 1. Average cell number in the *Nitrosomonas* sp. (grey bars) and *Nitrosococcus oceani* (white bars) cultures used in this study at the start (T_0) and end (T_{end}; 8 days for *Nitrosomonas* sp. and 12 days for *Nitrosococcus oceani*) of each experiment. Error bars are standard deviations from three replicate cultures.

4.2. Iodine and nitrogen speciation

Figure 2 shows that significant increases in the concentrations of IO_3^- (compared to media-only controls) were observed alongside NO_2^- production in both AOB cultures studied. In *Nitrosomonas* sp. (Figure 2ai and 2bi) there was a steady increase in IO_3^- concentrations throughout the experiment reaching a maximum of 19,921 (±4,754) nM by the end of the experiment (day 8). In contrast NO_2^- concentrations reached a maximum of 2,360 (±386) nM by day 6 and remained at around that level until the end of the experiment. In *Nitrosococcus oceani* (Figure 2aii and 2bii) IO_3^- concentrations increased rapidly during the initial stages of the experiment reaching 23, 943 (±8,568) nM by day 6. IO_3^- concentrations at the end of the experiment (day 12) were 16,365 (±7,603) nM. NO_2^- concentrations increased gradually throughout the experiment reaching 5,547 (±1,251) nM by day 12. There was larger variability in IO_3^- concentrations between replicates for *Nitrosococcus oceani* but despite this a clear increase in all replicates was observed.

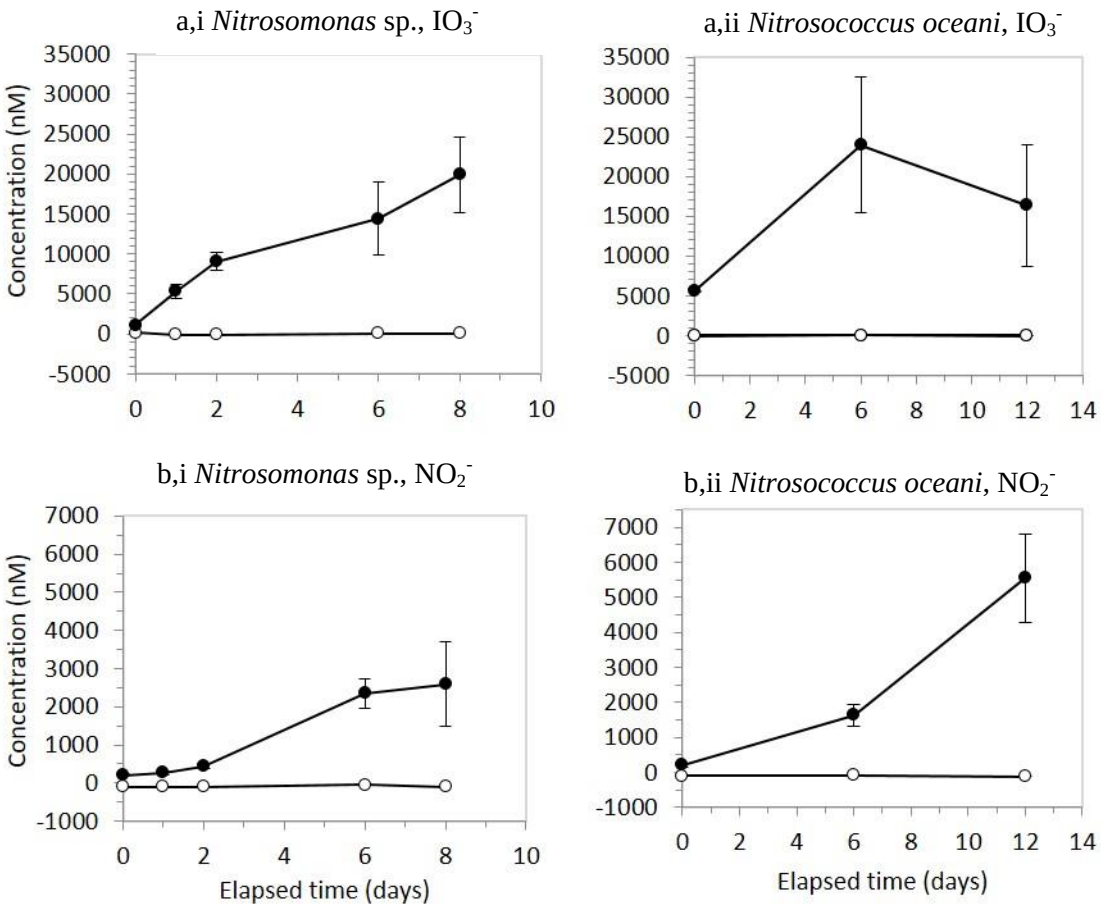

Figure 2. Changes in iodate (a) and nitrite (b) concentrations in cultures (closed symbols) and media-only controls (open symbols) for two cultures of ammonia-oxidising bacteria: i) *Nitrosomonas* sp.; and, ii) *Nitrosococcus oceani* supplied with 9-10 mM iodide and 7-8 mM NH_4^+. Error bars show the standard deviation of three replicate cultures.

Average production rates of IO_3^- and NO_2^- are presented in Table 1. In *Nitrosomonas* sp. average rates (±standard deviation) were 2,348 (±593) nM IO_3^- day^{-1} and 298 (±141) nM NO_2^- day^{-1}. In *Nitrosococcus oceani* averages rates were 897 (±640) nM IO_3^- day^{-1} and 445 (±99) nM NO_2^- day^{-1}. Minimum cell-normalised rates (based on the final cell density observed in each culture) were 15.69 (±4.71) fmol IO_3^- $cell^{-1}$ day^{-1} and 1.96 (±0.88) fmol NO_2^- $cell^{-1}$ day^{-1} for *Nitrosomonas* sp., and 11.96 (±6.96) fmol IO_3^- $cell^{-1}$ day^{-1} and 6.19 (±0.56) fmol NO_2^- $cell^{-1}$ day^{-1} for *Nitrosococcus oceani*. Molar ratios of iodate-to-nitrite production were 9.2±4.0 for *Nitrosomonas* sp. and 1.88±0.91 for *Nitrosococcus oceani.*

Table 1. Nitrite and iodate production rates (± standard deviations) observed in cultures of the ammonia-oxidising bacteria *Nitrosomonas* sp. and *Nitrosococcus oceani*. Cell-normalised values are a minimum as they are calculated using maximum cell densities.

	Nitrite		Iodate	
Culture	**nM day^{-1}**	**fmol cell^{-1} day^{-1}**	**nM day^{-1}**	**fmol cell^{-1} day^{-1}**
Nitrosomonas sp.	298 (±141)	1.96 (±0.88)	2,348 (±593)	15.69 (±4.71)
Nitrosococcus oceani	445 (±99)	6.19 (±0.56)	897 (±640)	11.96 (±6.96)

Figure 3 shows that, within error, a decline in I^- or NH_4^+ concentrations was not observed during either of the AOB experiments. Average starting I^- or NH_4^+ concentrations in *Nitrosomonas* sp. were 9.8 (±0.2) mM and 7.6 (±0.1) mM respectively. At the end of the experiment these values were 10.2 (±0.3) mM I^- and 7.7 (±0.1) mM NH_4^+. For *Nitrosococcus oceani* the start and end concentrations were 9.8 (±0.3) and 9.4 (±0.1) mM for I^- and 7.8 (±0.1) and 7.7 (±0.1) mM for NH_4^+. This result was expected as the average standard deviations associated with the observed concentrations of I^- or NH_4^+ (i.e. 0.1 to 0.3 mM) are at least an order of magnitude higher than the maximum levels of IO_3^- and NO_2^- observed in the culture experiments, i.e. very little of the initial stock of NO_2^- or NH_4^+ was oxidised during the experiments.

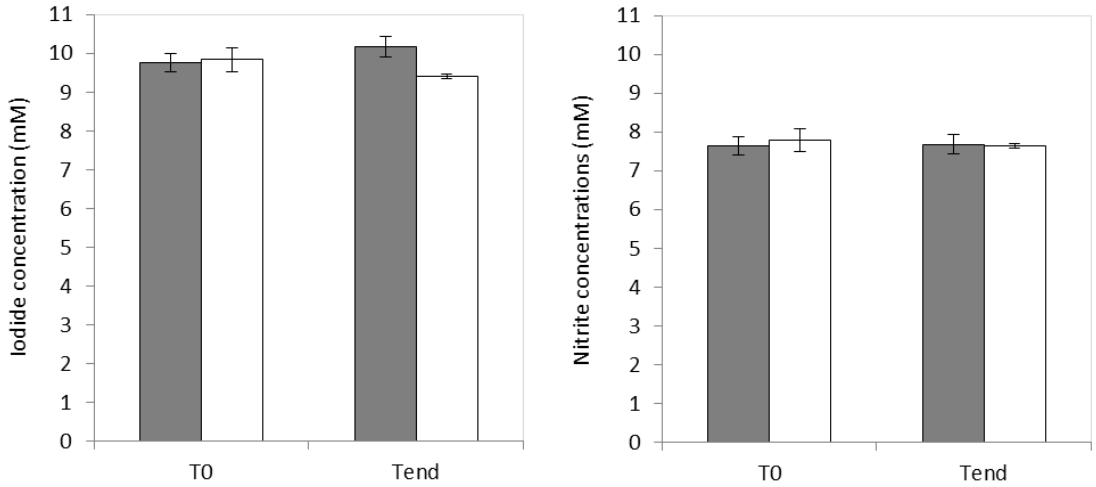

Figure 3. Start and end concentrations of a) iodide and b) ammonia in cultures of *Nitrosomonas* sp. (grey bars) and *Nitrosococcus oceani* (white bars). Error bars show the standard deviation of three replicate cultures.

296

297 **4.3 Iodine ocean cycling model results**

298 These results support the hypothesis that I^- oxidation is linked to ammonia oxidation and this process
299 has therefore been incorporated into the iodine model developed by Wadley *et al*. (2020) in the
300 companion paper. Such a link of iodide to ammonia oxidation means that I^- oxidation may be
301 sensitive to a change in ammonia oxidation rate such as anticipated to be likely to arise as a result of
302 ocean acidification (Beman *et al*., 2011). Figure 4 shows the change in global mixed layer I^-
303 concentration resulting from the modelled changes in the nitrification rate. It can be seen that a
304 reduction in the nitrification rate increases surface I^- concentrations by reducing I^- oxidation rate,
305 and *vice versa*. For changes of ±10%, the I^- changes are approximately linear. Changes are generally
306 greatest at low latitudes. The increase in I^- is greatest in the subtropical gyres, with maximum
307 changes of +30nM, corresponding to around a 25% increase in I^- for a 44% reduction in the
308 nitrification rate. It is in these regions that the fraction of ammonia subject to nitrification is greatest,
309 accounting for about half of the nitrogen cycled. Vertical mixing is also relatively weak, so oxidation
310 of I^- linked to nitrification is the dominant I^- sink, and the sensitivity to changes in the nitrification
311 rate is also greatest. At high latitudes nitrification is much less important, and strong seasonal
312 vertical mixing dominates the sink of iodide, so changes in the nitrification rate have little effect on I^-
313 concentrations.

314 The link between strong stratification, low nutrient concentrations and high nitrification rates is
315 consistent with the oceanic ecosystem having evolved to conserve nitrogen within the mixed layer. It
316 is possible that future heating of the upper layers of the ocean could increase stratification, and result
317 in an expansion of the subtropical regions subject to this regime. This in turn would result in a
318 reduced sink of I^- from vertical mixing, but an increase associated with nitrification. Further
319 modelling work would be required to quantify these competing processes.

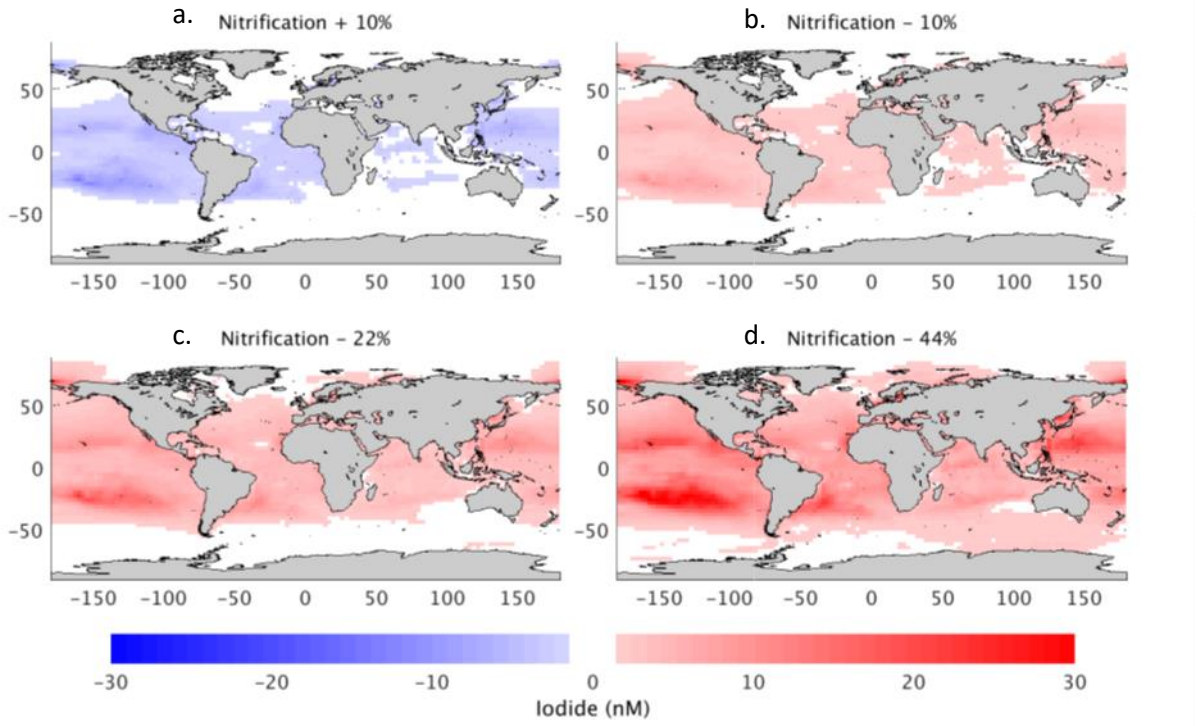

Figure 4. Modelled changes in surface I^- concentration (nM) resulting from a) +10%, b) -10%, c) -22% and d) -44% changes in the rates of nitrification. Negative percent values indicate a decline in the rate of nitrification and *vice-versa*. Negative values on the scale bar indicate a decrease in I^- concentrations and *vice versa*.

5. Discussion

5.1. Iodate production by ammonia-oxidising bacteria

Our results confirm that IO_3^- production occurs in cultures of the ammonia-oxidising bacteria *Nitrosomonas* sp. and *Nitrosococcus oceani* supplied with I^-, but not in cultures of nitrite oxidising bacteria. Coincident increases in NO_2^- (Figure 2) show that both cultures were actively oxidising ammonia throughout the experiments at rates of 1.96±0.0.88 fmol NO_2^- $cell^{-1}$ day^{-1} for *Nitrosomonas* sp. and 6.19±0.56 fmol NO_2^- $cell^{-1}$ day^{-1} for *Nitrosococcus oceani*. Whilst these cell-normalised oxidation rates are of the same order as those reported in the literature (e.g. 6-20 fmol NO_2^- $cell^{-1}$ day^{-1}; Ward *et al*., 1987; 1989) they are at the lower end. This is consistent with the approach taken here to calculate the rates by normalising to the final (highest) cell densities. It is also worth noting that the cultures were at an early stage of growth and had relatively low cell densities during the

experiment. This was done to avoid significant changes in pH in the bulk media which would impact inorganic iodine speciation (*Section 3.2*). The observation of an increase in IO_3^- concentrations alongside active biological ammonia oxidation supports previous studies (e.g. Truesdale *et al*., 2001; Zic *et al*., 2013) which have shown that high aqueous concentrations of IO_3^- are found in regions of enhanced nitrification, and provides the first direct confirmation of a biological basis for at least one mechanism of iodide oxidation

Whilst we did not set out to establish the mechanism for I^- to IO_3^- oxidation by marine nitrifiers, some speculations can be made. As I^- oxidation to IO_3^- requires the transfer of six electrons, it may occur in a series of one- or two- electron transfer steps. Initially, I^- may be oxidised to molecular iodine ($I^- \rightarrow I_2$), a reaction which is thermodynamically unfavourable at the pH of seawater (Luther *et al*., 1995). Further oxidation to IO_3^- by disproportionation ($I_2 \rightarrow HOI \rightarrow IO_3^-$) can occur spontaneously, but in seawater is subject to competition with reduction of I_2 by organic matter (Truesdale & Moore, 1992; Truesdale *et al*., 1995). It is not known whether the ammonia-oxidisers mediate just the first stage of I^- oxidation, with the observed IO_3^- production due to subsequent spontaneous reactions in the culture media, or if they are involved in driving the complete conversion of I^- to IO_3^-. However, bacteria which just oxidise I^- to I_2 have been isolated from seawater aquaria (Gozlan, 1968), I^--rich natural gas brine waters (Amachi *et al*., 2005) and marine environmental samples (Fuse *et al*., 2003; Amachi *et al.*, 2005).

The observed IO_3^- production is either linked to the nitrification process itself or associated with other metabolic activities of the AOB studied. Truesdale *et al.* (2001) has proposed that I^- oxidation to IO_3^- would be energetically advantageous for chemoautotrophic AOB. In that case the key enzymes used to obtain energy during the oxidation of NH_4^+ to NO_2^- (ammonia monooxygenase [AMO] and hydroxylamine oxidoreductase [HAO]) could also have the potential to use I^- as a

363 substrate. The observed IO_3^--to-NO_2^- molar production rates (9.2±4.0 for *Nitrosomonas* sp. and
364 2.3±1.1 for *Nitrosococcus oceani*) are intriguing. If AMO/HAO are involved, this suggests that the
365 enzymes have higher affinities for I^- than NH_4^+/NH_2OH given the similar concentrations of I^- and
366 NH_4^+ used in the experiments. Other enzymes that have been implicated in I^- oxidation include the
367 chloroperoxidases (Thomas & Hager, 1968) but we do not know if they occur in AOB. The exact
368 metabolic pathway driving the observed IO_3^- production and its controls (i.e. substrate concentrations,
369 light intensity) will need to be determined in future work. To establish if such further
370 experimentation is warranted we need to explore whether the link between nitrification and I^-
371 oxidation is likely to be an important part of inorganic iodine cycling in seawater.
372
373 **5.2. Implications for inorganic iodine speciation in the oceans**
374 Our culture studies suggest that the molar rate of I^- oxidation (IO_3^- production) is ~2-9 times higher
375 than that for ammonia oxidation (nitrification). Ammonia oxidation rates in seawater range from
376 below detection to 10^2 nM day^{-1} (Table 2). Literature estimates of the rate of I^- oxidation in the
377 marine environment range from ~4 to 670 nM $year^{-1}$ or 0.01 to 1.84 nM day^{-1} (reviewed in Chance *et*
378 *al*., 2014). If the oxidation molar ratios observed in this study (~2-9) are representative, predicted
379 rates of I^- oxidation are in-line (i.e. 2-9 times higher) with the lower end of observed ammonia
380 oxidation rates (Table 2).
381
382 **Table 2.** Ammonia-oxidation rates measured in a range of ocean regions.
383

Study	Location	Rate (nM day^{-1})
Newell *et al*. (2011)	Arabian Sea, Indian Ocean	undetected to 21.6
Smith *et al*. (2015)	Northeast Pacific	< 0.01 to 90
Peng *et al*. (2015)	Eastern tropical north Pacific	< 1 to 8.6
Newell *et al.* (2013)	Subtropical Atlantic, Sargasso Sea (BATS)	< 2
Lam *et al*. (2007)	Black Sea	7-24
Beman *et al*. (2012)	Gulf of California, eastern tropical north Pacific	0-348

384
385

Truesdale *et al.* (2001) derive likely I^- oxidation (or IO_3^- production) rates for the near surface Black Sea using an iodine budget and this allows us to examine the potential importance of the link between nitrification and I^- oxidation on a local scale. They predict a minimum I^- oxidation flux of 3.89×10^{-4} mol I m^{-2} $year^{-1}$ which is an average of 0.02 nM day^{-1} at a mixed-layer depth (MLD) of 50 m or 0.11 nM day^{-1} at a MLD of 10 m. Lam *et al.* (2007) report an AOB abundance of ≤1,400 cells mL^{-1} in the Black Sea. If we apply a cell density of 1,400 AOB cells mL^{-1} to the average cell-normalised rates of IO_3^- production observed in this study (Table 1) we derive I^- oxidation rates of ~20 nM d^{-1}. This is clearly much higher than the rates suggested in Truesdale *et al*. (2001). This discrepancy could be explained in a number of ways. Firstly, Lam *et al.* (2007) state that net nitrification only takes place within a narrow depth range of the Black Sea water column (i.e. between 71 and 81 m) and, the I^- oxidation values derived in Truesdale *et al*. (2001) are minimum values. It is also possible that the AOB studied here have a higher capacity for I^- oxidation (per unit ammonia-oxidised) than other ammonia-oxidisers or that our culture conditions (e.g. substrate availability) promoted higher I^- oxidation rates than would be observed in marine systems. For example, ammonia-oxidising Archaea (AOA), which can outnumber known bacterial ammonia oxidisers by orders of magnitudes in environments such as the marine water-column (reviewed by Schleper & Nicol, 2010), may have a very different capacity for I^- oxidation compared to the AOB studied here. Further studies are needed to establish the relationship between ammonia- and I^- oxidation in the marine environment.

5.3. Potential implications for future oceanic inorganic iodine distributions

Results from our iodine cycling model (Wadley *et al*., 2020) suggest that the predicted decrease in the rate of nitrification under ocean acidification (Beman *et al*., 2011) could lead to an increase in the concentration of sea surface I^- across most of the world's oceans. The largest changes are likely to occur in regions such as the sub-tropical gyres where, according to our model, the I^- loss process is a

411 dominant part of the inorganic iodine cycle. At high latitudes where a dominant loss process is
412 removal from the mixed layer by seasonal mixing the changes are not as great but still significant.
413 Zonal mean changes in I^- (Figure 5) reflect this, with a 0.27 nM increase in annual mean I^- for each
414 percent decrease in the nitrification rate in the subtropical gyres, and around half this at the equator.
415 There is a marked asymmetry at higher latitudes, with a 0.06 nM / % increase between 60^{o}N and
416 80^{o}N, where summertime iodide concentrations are predicted to be high (there are currently no
417 observations to verify this), whereas in the Southern Ocean changes are predicted to be < 0.02 nM
418 / %. The global mean sensitivity is 0.13 nM increase in I^- per % decrease in nitrification. Carpenter *et*
419 *al.* (2013) show that I_2 emissions due to ozone deposition increase near linearly with I^- concentration.
420 Hence, the predicted changes to sea surface I^- fields under future ocean acidification could have a
421 major impact on ozone deposition to the sea surface, atmospheric chemistry and resulting sea-air
422 iodine emissions.

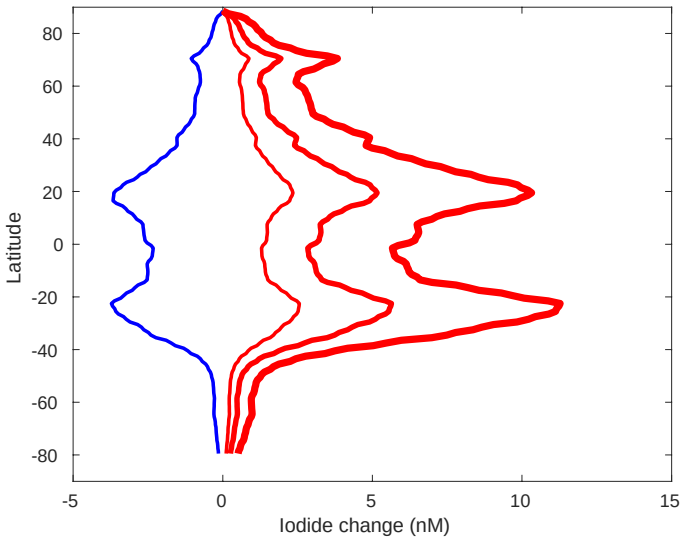

423

424 **Figure 5.** Zonal mean changes in iodide concentration for +10% (blue), -10% (red thin), -22% (red)
425 and -44% (red thick) changes in nitrification modelled using the ocean iodine cycling model
426 presented in Wadley *et al.* (2020).

427

428 **5.4.Conclusions**

This study has shown that I^- oxidation to IO_3^- occurs in cultures of ammonia oxidising (nitrifying) bacteria, but not nitrite oxidising bacteria. Our calculations suggest that I^- oxidation by AOB could be an important control on inorganic iodine speciation in seawater, but to confirm this further study is needed on a wider range of ammonia-oxidisers including ammonia oxidising archaea (AOA). Simulations from our iodine cycling model suggest that changes in nitrification rate, such as those predicted to occur under acidification (Beman *et al*., 2011), could have an important impact on sea surface I^- fields. A decrease in marine nitrification under ocean acidification could lead to higher sea surface I^-, especially in regions such as the sub-tropical gyres where downward mixing is limited. In turn, this could lead to an increase in ozone deposition to the sea surface and sea-air iodine emissions with potentially major implications for atmospheric chemistry and air quality.

Acknowledgements

The authors have no financial conflicts of interest with the research in this paper. This research was funded under NERC grant no. NE/N01054X/1. The work undertaken by EB within this study was supported by the University of York Laidlaw Scholarship. We thank Eva Spieck (University of Hamburg, Germany) for supplying the nitrite oxidising bacteria (NOB) cultures used in our preliminary experiments. The data presented in this manuscript will be made available at the British Oceanographic Data Centre (BODC), archiving the data is underway.

References

Amachi, S., Muramatsu, Y., Akiyama, Y., Miyakzaki, K., Yoshiki, S., Hanada, S. *et al*. (2005) Isolation of iodide-oxidizing bacteria from iodide-rich natural gas brines and seawaters, *Microbial Ecology*, *49*, 547-557

Amachi, S. (2008) Microbial contribution to global iodine cycling: volatilization, accumulation, reduction, oxidation, and sorption of iodine, *Microbes Environment*, 23 269-276

Beman, J. M., Chow, C.-E., King, A. L., Feng, Y., Fuhrman, J. A., Andersson, A., *et al*. (2011). Global declines in oceanic nitrification rates as a consequence of ocean acidification, *Proceedings of the National Academy of Sciences*, 108, 208-213, https://doi.org/10.1073/pnas.1011053108

Beman, J.M., Popp, B. N. & Alford, S. E. (2012) Quantification of ammonia oxidation rates and ammonia-oxidizing archaea and bacteria at high resolution in the Gulf of California and eastern tropical North Pacific Ocean, *Limnology and Oceanogr*aphy, 57, 712-726

Bluhm, K., Croot, P., Wuttig, K., & Lochte, K. (2010). Transformation of iodate to iodide in marine phytoplankton driven by cell senescence, *Aquatic Biology*, 11(1), 1-15, https://doi.org/10.3354/ab00284

Carpenter, L. J. (2003) Iodine in the marine boundary layer, *Chemistry Reviews*, 103, 4953-4962

Carpenter, L. J., Shaw, M. D., Parthipan, R., Wilson, J., MacDonald, S. M., Kumar, R. *et al*. (2013). Atmospheric iodine levels influenced by sea surface emissions of inorganic iodine, *Nature Geoscience*, 6 (2). 108 – 111, ISSN 1752-0894

Chance, R., Weston, K., Baker, A. R., Hughes, C., Malin, G., Carpenter, L. *et al*. (2010). Seasonal and interannual variation of dissolved iodine speciation at a coastal Antarctic site, *Marine Chemistry*, 118, 171-181, https://doi.org/10.1016/j.marchem.2009.11.009

Chance, R., Malin, G., Jickells, T. D., & Baker, A. R. (2007). Reduction of iodate to iodide by cold water diatom cultures, *Marine Chemistry*, 105, 169-180, https://doi.org/10.1016/j.marchem.2006.06.008

Chance, R., Baker, A. R., Carpenter, L., & Jickells, T. D. (2014). The distribution of iodide at the sea surface, *Environmental Science: Processes & Impacts*, 16, 1841-1859, https://doi.org/10.1039/C4EM00139G

Chapman P. & Liss, P. S. (1977) The effect of nitrite on the spectrophotometric determination of iodate in seawater, *Marine Chemistry*, 5, 243-249.

Dickson, A. G., Sabine, C. L. & Christian, J. R. (Eds.) (2007) Guide to Best Practices for Ocean CO_2 Measurements. *PICES Special Publication 3*. 191 pp.

521 Fuse, H., Inoue, H., Murakami, K., Takimura, O. & Yamaoka, Y. (2003). Production of free and
522 organic iodine by *Roseovarius spp*., *FEMS Microbiological Letters*, 229, 189-194,
523 https://doi.org/10.1016/S0378-1097(03)00839-5

524

525 Gozlan, R.S. (1968) Isolation of iodine-producing bacteria from aquaria, *Antonie Van Leeuwenhoek*,
526 34, 226

527

528 Hung, C-C., Wong, G. T. F. & Dunstan, W. M. (2005) Iodate reduction activity in nitrate reductase
529 extracts from marine phytoplankton, *Bulletin of Marine Science*, 76, 61-72.

530

531 Jickells, T. D., Boyd, S. S., & Knap, A. H. (1988). Iodine cycling in the Sargasso Sea and the
532 Bermuda inshore waters, *Marine Chemistry*, 24, 61-82, doi:10.1016/0304-4203(88)90006-0.

533

534 Koops H. and Pommerening-Röser, A. (2001). Distribution and ecophysiology of the nitrifying
535 bacteria emphasising cultured species, *FEMS Microbiology Ecology*, 37, 1-9

536

537 Lam, P., Jensen, M. M., Lavik, G., McGinnis, D. F., Müller, B., Schubert, C. J. *et al*. (2007)
538 Linking crenarchaeal and bacterial nitrification to anammox in the Black Sea. *Proceedings of the*
539 *National Academy of Science*, 104 (17), 7104-7109

540

541 Li H., Daniel, B., Creeley, D., Grandbois, R., Zhang, S., Xu, C. *et al*. (2014). Superoxide production
542 by a Manganese-oxidising Bacterium Facilitates Iodide Oxidation, *Applied and Environmental*
543 *Microbiology*, 80 (9), 2693-2699

Lino, T., Ohkuma, M., Kamagata, Y. & Amachi, S. (2016) *Iodidimonas muriae* gen. nov., sp. nov., an aerobic iodide-oxidizing bacterium isolated from brine of a natural gas and iodine recovery facility, and proposals of *Iodidimonadaceae* fam. nov., *Iodidimonadales* ord. nov., *Emcibacteraceae* fam. nov. and *Emcibacterales* ord. nov., *International Journal of Systematic and Evolutionary Microbiol*ogy, 66(12), 5016-5022 https://doi.org/10.1099/ijsem.0.001462

Long, A., Dang, A., Xiao, H., & Yu, X. (2015). The Summer Distribution of Dissolved Inorganic Iodine along 18^{o}N in the South China Sea, *Journal of Marine Science: Research & Development*, 5, 169, doi:10.4172/2155-9910.1000169

Newell, S. E., Babbin, A. R., Jayakumar, A. & Ward, B. B. (2011) Ammonia oxidation rates and nitrification in the Arabian Sea, *Global Biogeochemical Cycles*, 25, https://doi.org/10.1029/2010GB003940

Newell, S. E., Fawcett, S. E. & Ward B. B. (2013) Depth distribution of ammonia oxidation rates and ammonia-oxidizer community composition in the Sargasso Sea, *Limnology and Oceanography*, 58, 1491-1500

Norwitz G. & Keliher, P. N. (1984). Spectrophotometric Determination of Nitrite with Composite Reagents Containing Sulphanilamide, Sulphanilic Acid or 4-Nitroaniline as the Diazotisable Aromatic Amine and N-(1-Naphthyl) ethylenediamine as the Coupling Agent, *Analyst*, 109, 1281-1286

O'Dowd C., Jimenez, J. L., Bahreini, R., Flagan, R. C., Seinfield, J. H., Hàmeri, K. *et al* (2002). Marine aerosol formation from biogenic iodine emissions, *Nature*, 417, 632-636

Peng, X., Fuchsman, C. A., Jayakumar, A., Oleynik, S., Martens-Habbena, W., Devol, A. H., *et al*. (2015) Ammonia and nitrite oxidation in the Eastern Tropical North Pacific, *Global Biogeochemical Cycles*, 29, 2034-2049

Schulz, K. G., Barcelos e Ramos, J., Zeebe, R. E. & Riebesell, U. (2009). CO_2 perturbation experiments: similarities and differences between dissolved organic carbon and total alkalinity manipulations, *Biogeosciences*, 6, 2145-2153

Smith, J. A., Damashek, J., Chavez, F. P. & Francis, C. A. (2015) Factors influencing nitrification rates and the abundance and transcriptional activity of ammonia-oxidizing microorganisms in the dark northeast Pacific Ocean, *Limnology and Oceanography, 61*, 596-609

Schleper C. & Nicol, G.W. (2010) Ammonia-oxidising archaea physiology, ecology and evolution. *Advances in Microbial Physiology, 57,* 1-41

Sherwen, T., Evans, M. J., Carpenter, L. J., Andrews, S. J., Lidster, R. T., Dix, B. *et al*. (2016). Iodine's impact on tropospheric oxidants: a global model study in GEOS-Chem, *Atmospheric Chemistry and Physics*, 16, 1161-1186, https://doi.org/10.5194/acp-16-1161-2016

589

590 Thomas, J. A. & Hager, L. P. (1968) The peroxidation of molecular iodine to iodate by
591 chloroperoxidase, *Biochemica Biophysica Research Communications*, 32, 770-775

592

593 Truesdale, V. W. & Spencer, C. P. (1974) Studies on the determination of inorganic iodine in sea
594 water, *Marine Chemistry*, 2, 33–47

595

596 Truesdale, V. W. & Moore, R. M. (1992) Further studies on the chemical reduction of molecular
597 iodine added to seawater, *Marine Chem*istry, 40, 199–213

598

599 Truesdale, V. W. & Luther II, G. W. (1995) Molecular iodine reduction by natural and model
600 organic substances in seawater, *Aquatic Geochem*emistry, 1, 89-104

601

602 Truesdale, V. W., Watts, S. F., & Rendell, A. R. (2001). On the possibility of iodide oxidation in the
603 near-surface of the Black Sea and its implications to iodine in the general ocean, *Deep-Sea Research*,
604 48, 2397-2412, https://doi.org/10.1016/S0967-0637(01)00021-8

605

606 Wadley, M. R., Stevens, D. P., Jickells, T. D., Hughes, C., Chance, R., Hepach, H. et al. (2020) A
607 Global Model for Iodine Speciation in the Upper Ocean, Revised manuscript Submitted to *Global*
608 *Biogeochemical Cycles*, Unpublished manuscript available at
609 https://www.essoar.org/doi/10.1002/essoar.10502078.2

610

611 Ward, B. B. (1987) Nitrogen transformations in the Southern California Bight, *Deep-Sea Res*earch,
612 34, 785–805

613

614 Ward, B. B., Glover, H. E., & Lipschulz, F. (1989) Chemoautotrophic activity and nitrification in the
615 oxygen minimum zone off Peru, *Deep-Sea Research A,* 36, 1031-1036

616

617 Wong, G. T. F. (1991). The marine geochemistry of iodine, *Reviews in Aquatic Science*, 4, 45-73.

618

619 Yool, A., Martin, A. P., Fernandez, C., & Clark, D. R. (2007). The significance of nitrification for
620 oceanic new production, *Nature,* 447, 999-1002, doi:10.1038/nature05885

621

622 Zic, V., Caric, M & Ciglenecki, I. (2013). The impact of natural water column mixing on iodine and
623 nutrient speciation in a eutrophic anchialine pond (Rogoznica Lake, Croatia), *Estuarine, Coastal and*
624 *Shelf Science*, 133, 260-272, https://doi.org/10.1016/j.ecss.2013.09.008

625